ACS APPLIED MATERIALS & INTERFACES

Research Article

www.acsami.org

Nonconjugated Anionic Polyelectrolyte as an Interfacial Layer for the Organic Optoelectronic Devices

Gyeong Eun Lim,[†] Ye Eun Ha,[†] Mi Young Jo,[†] Juyun Park,[‡] Yong-Cheol Kang,[‡] and Joo Hyun Kim*,[†]

[†]Department of Polymer Engineering and [‡]Department of Chemistry, Pukyong National University, Busan 608-739, Korea

Supporting Information

ABSTRACT: A nonconjugated anionic polyelectrolyte, poly(sodium 4-styrenesulfonate) (PSS-Na), was applied to the optoelectronic devices as an interfacial layer (IFL) at the semiconducting layer/cathode interface. The ultraviolet photoelectron spectroscopy and the Kelvin probe microscopy studies support the formation of a favorable interface dipole at the organic/cathode interface. For polymer light-emitting diodes (PLEDs), the maximum luminance efficiency (LE_{max}) and the turn-on voltage (V_{on}) of the device with a layer of PSS-Na spin-coated from the concentration of 0.5 mg/mL were 3.00 cd/A and 5.5 V, which are dramatically improved than those of the device without an IFL (LE_{max} = 0.316 cd/A, V_{on} = 9.5 V). This suggests that the PSS-Na film at the emissive layer/cathode interface improves the electron injection ability. As for polymer solar cells (PSCs), the power conversion efficiency (PCE) of the device with a layer of PSS-Na spin-coated from the concentration of 0.5 mg/mL was 2.83%, which is a 16% increase compared to that of the PSC without PSS-Na. The PCE improvement is mainly due to the enhancement of the short-circuit current (12% increase). The results support that the electron collection and transporting increase by the introduction of the PSS-Na film at the photoactive layer/cathode interface. The improvement of the efficiency of the PLED and PSC is due to the reduction of the Schottky barrier by the formation of a favorable interface as well as the better Ohmic contact at the cathode interface.

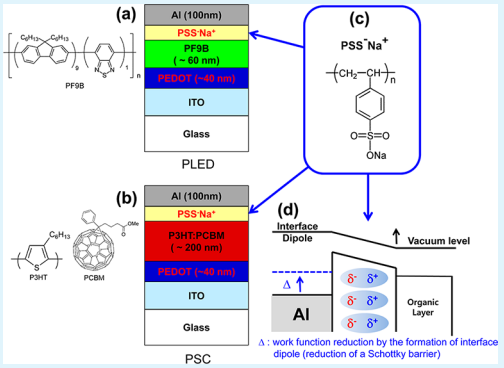

KEYWORDS: *nonconjugated anionic polyelectrolyte, interfacial layer, electron transporting/injecting layer, optoelectronic device, interface dipole, electrical contact resistance*

INTRODUCTION

Recently, the organic optoelectronic devices, such as polymer light-emitting diodes (PLEDs) and polymer solar cells (PSCs), have been extensively studied because of the possibility of their application in flexible devices and low fabrication cost.[1−4] The charge transporting and injecting/collecting properties are important factors for influencing the performances of the devices. These are strongly related to the interfacial properties between the emissive layer (EML) (or photoactive layer (PAL)) and the cathode or the anode.[5] A thin layer of PEDOT:PSS,[6] thermally curable arylamine derivatives,[7−12] and self-assembled monolayers (SAMs) modification[13−15] were mainly used for improving the interface properties between the EML (or PAL) and the anode to achieve highly efficient devices. For a cathode side, highly efficient devices are then achieved by the introduction of low work function metal electrodes. However, low work function metals are very sensitive to oxygen or moisture under the ambient condition. The utilization of quite stable metal electrodes, such as Al or Ag, seemed to be unavoidable, although the devices based on Al or Ag show poor performances. One of the potential methods to improve interfacial property is the introduction of a buffer layer between the EML (or PAL) and the metal electrode. The introduction of a poly(ethylene oxide) (PEO),[16] cationic π-conjugated polymer electrolytes (CPEs) with quaternary ammonium salt,[17−20] alcohol-soluble neutral conjugated polymers (P-OH),[21] nonconjugated polymer electrolytes based on viologen derivatives (PVs),[22,23] or solution processable n-type metal oxides, such as TiO_x[24] and ZnO,[25] have been reported as an interfacial layer (IFL) to improve the performances of the optoelectronic devices. The efficiency of the devices with these materials as an IFL at the active layer/metal cathode interface was dramatically improved by the formation of a favorable interface dipole, which reduces the work function of the metal as well as the electrical contact resistance.

The anionic CPEs with sulfonate[26,27] and the nonconjugated cationic polyelectrolytes[22,23] were used as an electron transporting and injecting/collecting layer for PLEDs and PSCs. Therefore, a nonconjugated anionic polyelectrolyte, such as poly(sodium 4-styrenesulfonate) (PSS-Na) (Figure 1c), might be used as an IFL between the EML (or PAL) and the cathode. PSS-Na is a well-known commercially available nonconjugated anionic polyelectrolyte and very soluble in polar protic solvents, such as water or water/alcohol mixtures. The solubility of PSS-Na in polar protic solvents offers the options available for the utilization of an IFL in the optoelectronic applications. A

Received: February 6, 2013
Accepted: June 19, 2013
Published: June 19, 2013

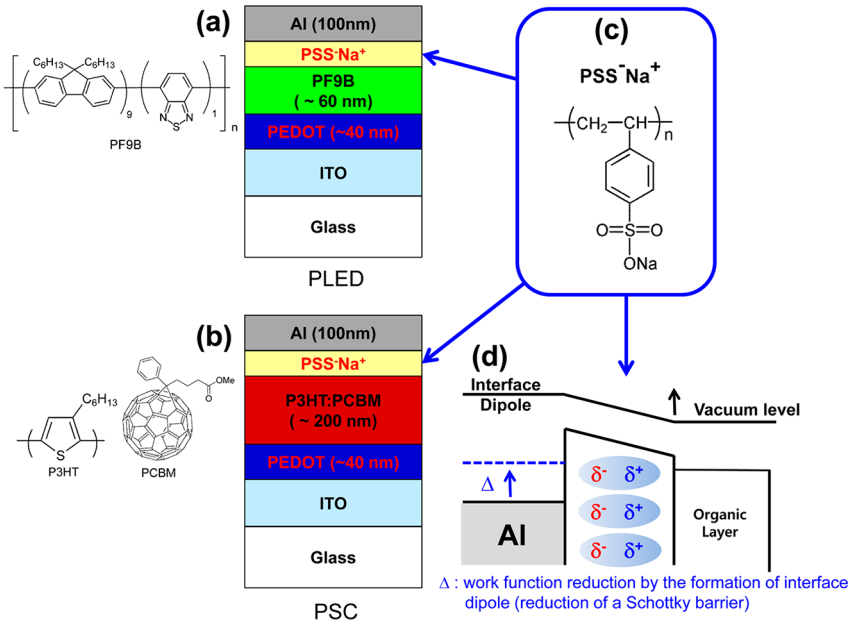

Figure 1. Device structures and the chemical structures of materials used in the device fabrications: (a) PLED, (b) PSC. (c) The chemical structure of PSS-Na. (d) The proposed work function reduction scheme by the formation of a favorable interface dipole between the organic layer and the cathode (Δ: the work function reduction (the reduction of a Schottky barrier) by the PSS-Na thin film. Φ: the work function of a thin film of PSS-Na coated Al).

monolayer of PSS-Na can be absorbed on a substrate with a positively charged surface; then the surface charge is reversed. A layer of cationic polyelectrolyte can be absorbed on a reversed charged surface. By repeating both steps successively, alternating multilayer assemblies of both anionic and cationic polyelectrolytes can be obtained.[28] In this case, there is no discernible permanent dipole. The surface of a thin layer of PSS-Na coated EML (or PAL) will be negatively charged because the hydrophobic EML (or PAL) will push away the ion pairs from a surface of the EML (or PAL). As for anionic conjugated polyelectrolytes for an IFL, the mobile counterions will move to the cathode to form a strong favorable dipole and the polymer with anionic charge will not move; then a double layer between free counterions and the cathode is obtained to make better electron injection.[26] We believe that the similar features are expected in PSS-Na. Therefore, the interface dipole will be generated between the EML (or PAL) by the permanent dipole moment. In this paper, we report the characteristics of the optoelectronic devices with a very thin layer of PSS-Na as an IFL between the EML (or PAL) and the cathode. As illustrated in Figure 1d, a very thin layer of PSS-Na will improve the electron transporting and injecting/collecting property by the formation of a favorable interface dipole and the reduction of electrical contact resistance. To the best of our knowledge, the PLEDs and PSCs with the PSS-Na film as an IFL have never been tested and reported before.

EXPERIMENTAL SECTION

Materials. Chemicals were purchased from Aldrich Chemical Co. and Alfa Aesar and were used as received unless otherwise described. Poly(sodium 4-styrenesulfonate) (Cat. No. 45851, M_w = 75 000 g/mol) and poly(4-styrenesulfonic acid) were purchased from Alfa Aesar. Regioregular P3HT (Cat. No. 4002-EE) and PCBM (Cat No. nano-cPCBM-BF) were purchased from Rieke Metals Inc. and nano-C, Inc., respectively. PF9B was used as an EML and synthesized according to the literature procedures.[29] PF9B is a random copolymer based on 90 mol % of 9,9-dihexylfluorene and 10 mol % of 2,1,3-benzothiadiazole.

Measurements. The thickness of the film was measured by an Alpha-Step IQ surface profiler (KLA-Tencor Co.). The work function measurements were carried out using a UPS (VG Scientific Co.) with a He I source ($h\nu$ = 21.2 eV) at a pressure of 1×10^{-8} Torr. A −3 V was applied to a sample during the measurements to distinguish between the analyzer and the sample cutoff. We also performed the Kelvin probe (KP) measurements (McAllister Technical Services, KP 6500) of the contact potential difference between the sample and the KP tip to confirm the effective work function. The KP tip work function was 5.203 ± 0.011 eV. The water contact angle was measured using a KRUSS Model DSA 100. Atomic force microscope (AFM) images were taken on a Digital Instruments (Multi ModeTM SPM). AFM images were obtained by the tapping mode and at a scan rate of 2 Hz. The $J-V$ measurements under the 1.0 sun (100 mW/cm^2) condition from a 150 W Xe lamp with an AM 1.5G filter were performed using a KEITHLEY Model 2400 source-measure unit. A calibrated Si reference cell with a KG5 filter certified by the National Institute of Advanced Industrial Science and Technology was used to confirm the 1.0 sun condition.

Fabrication of PLEDs and PSCs. For fabrication of PLEDs with a structure of ITO/PEDOT/EML (PF9B)/PSS-Na/Al, a thickness of 40 nm of PEDOT:PSS (Baytron P, diluted with 2-propanol 1:2 v/v) was spin-coated on a precleaned indium tin oxide (ITO) glass substrate (sheet resistance = 15 ohm/sq). After being baked at 150 °C for 10 min under the air, an emissive polymer solution (10 mg/mL in toluene) was spin-coated onto the PEDOT:PSS layer at 2000 rpm for 60 s. Prior to spin-coating, the emissive polymer solution was filtered through a 0.45 μm membrane filter. The typical thickness of the EML was 60 nm. Before cathode deposition, the IFL of PSS-Na was prepared by spin-coating with a different concentration of solution of PSS-Na at 4000 rpm for 60 s. The typical thickness of a PSS-Na film was less than 5 nm. The thickness of the PSS-Na layer was controlled by the concentration of the PSS-Na solution. The Al layer was deposited with a thickness of 100 nm through a shadow mask with a device area of 0.13 cm^2 at 2×10^{-6} Torr.

For fabrication of PSCs with a structure of ITO/PEDOT/PAL (P3HT:PCBM)/PSS-Na/Al, the deposition of a PEDOT:PSS layer is the same as the fabrication of PLEDs. After being baked at 150 °C for 10 min under the air of a PEDOT:PSS layer, the PAL was spin-cast from the blend solution of P3HT and PCBM (20 mg of P3HT and 20

dx.doi.org/10.1021/am400478b | ACS Appl. Mater. Interfaces 2013, 5, 6508−6513

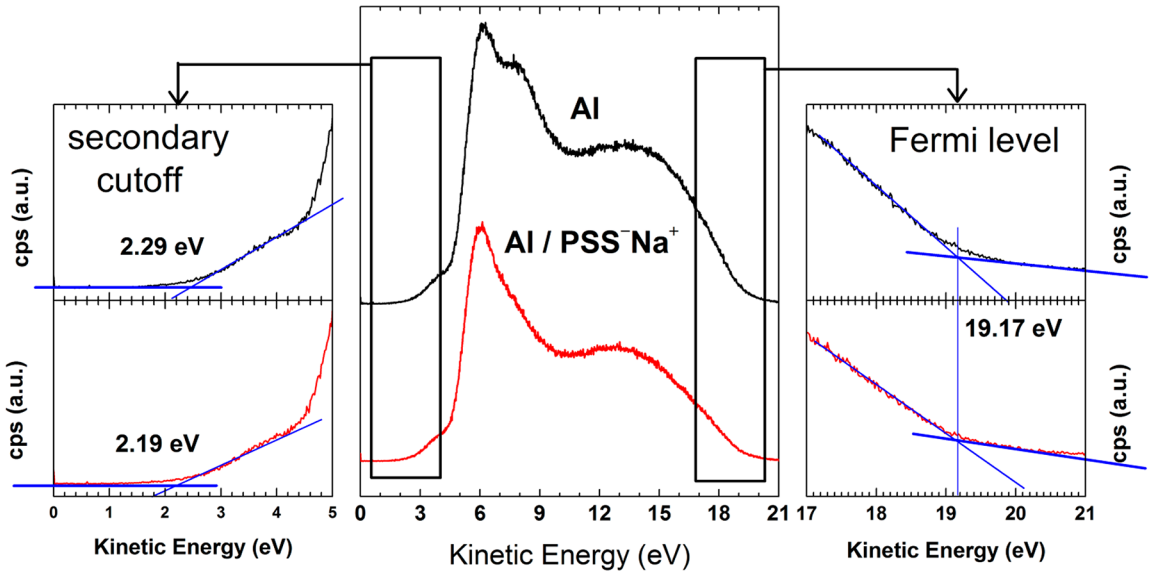

Figure 2. UPS spectra of Al and PSS-Na coated Al.

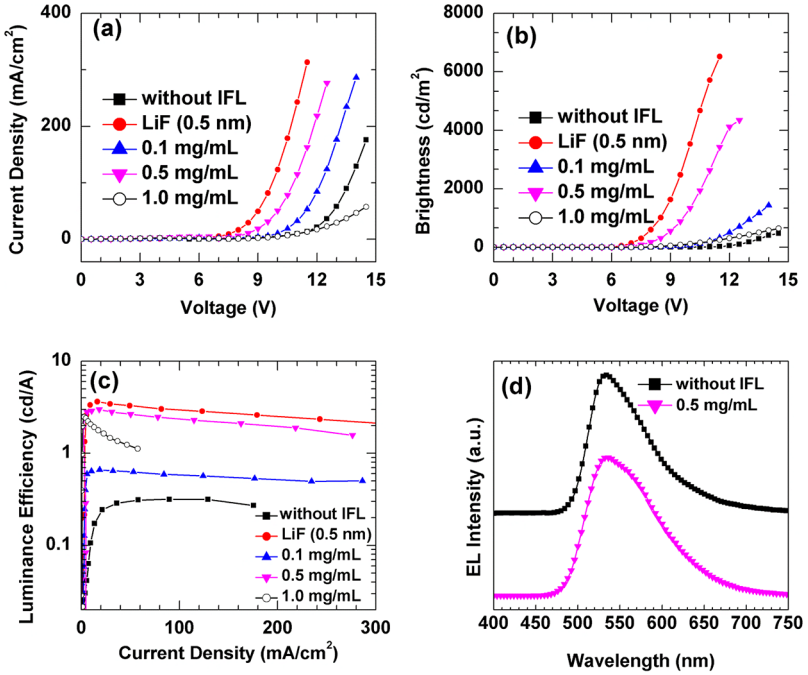

Figure 3. (a) Current density−voltage, (b) brightness−voltage, and (c) luminance efficiency−current density curves and (d) electroluminescence spectra (offset for clarity) of PLEDs (filled rectangle: without IFL; filled circle: a 0.5 nm thick LiF as an IFL; filled triangle: PSS-Na coated from the solution of 0.1 mg/mL; filled reverse triangle: PSS-Na coated from the solution of 0.5 mg/mL; circle: PSS-Na coated from the solution of 1.0 mg/mL).

mg of PCBM dissolved in 1 mL of *o*-dichlorobenzene (ODCB)) at 600 rpm for 40 s and then dried in a covered Petri dish for 1 h. Prior to spin-coating, the photoactive solution was filtered through a 0.45 μm membrane filter. The typical thickness of the PAL was 200 nm. The deposition procedures of the IFL and cathode were the same as the fabrication of PLEDs. After the cathode deposition, the device was thermally annealed at 150 °C for 20 min in the glovebox (N_2 atmosphere).

RESULTS AND DISCUSSION

Characterization of the Al/PSS-Na Interface. PSS-Na has sodium sulfate salt on the side chain, which is a very polar and has a permanent dipole. Therefore, as illustrated in Figure 1, the work function of a thin layer of PSS-Na coated Al (Φ) cathode might be lower than that of the Al cathode without PSS-Na because of the formation of a favorable interface dipole. We performed ultraviolet photoelectron spectroscopy (UPS) to measure the work function of the Al and the PSS-Na coated Al. As shown in Figure 2, the work function was estimated from the secondary cutoff energy and the Fermi level in the UPS spectrum. The work functions of the PSS-Na coated Al and the Al figured out from the UPS spectra were 4.22 and 4.32 eV, respectively. The work function of a thin layer of PSS-Na coated Al was smaller than that of Al. To crosscheck the work function variation by the PSS-Na thin film, we performed the

dx.doi.org/10.1021/am400478b | ACS Appl. Mater. Interfaces 2013, 5, 6508−6513

Table 1. Performances of the PLEDs

	V_{on}[a] (V)	LE_{max}[b] (cd/A) at V	LE_{100}[c] (cd/A)	B_{max}[d] (cd/m^2) at V
without IFL	9.5	0.316	0.282	476 at 14.5
LiF (0.5 nm)	6.0	3.64	1.97	6518 at 11.5
IFL (0.1 mg/mL)	7.0	0.660	0.649	1436 at 14.0
IFL (0.5 mg/mL)	5.5	3.00	2.56	4348 at 12.5
IFL (1.0 mg/mL)	7.5	2.49	2.47	643 at 14.5

[a]Turn-on voltage is defined as the voltage at a brightness of 1 cd/m^2. [b]Maximum luminance efficiency. [c]Luminance efficiency at a brightness of 100 cd/m^2. [d]Maximum brightness.

measurements of the work function by the Kelvin probe microscopy (KPM), which is a very good instrumental analysis for investigating the work function near the metal/organic interface.[30−34] The effective work function of a thin layer PSS-Na coated Al obtained from the KPM was 4.16 ± 0.03 eV, which is smaller than the effective work function of PSS-Na coated Al (4.30 ± 0.02 eV). The KPM results also support that the work function of the Al cathode is reduced by the formation of an interface dipole. Generally, a large Schottky barrier inhibits the facile transport/injection of electrons at the organic (or polymer) semiconductor/Al interface. From the UPS and KPM results, the reduction of a Schottky barrier was small (ca. 0.1 eV) compared to the case with the PEO, CPEs, P-OH, and PVs as an IFL (higher than 0.2 eV).[16−23,26,27] However, the more efficient transport/injection of electrons is expected in the device with the thin film of PSS-Na as an IFL. It is well-known that the property of solvents for IFL materials and the wetting property of an IFL on the semiconducting layer are important factors for governing the performances of the optoelectronic devices.[22,35,36] From the our experience, the amount of water in the solvent for IFL materials should be less than 30%.[22,23] Fortunately, the solubility of PSS-Na in the water/methanol mixed solvent (1:9 by volume) of was up to 2 mg/mL. The static water contact angles of the active layer (P3HT:PCBM) and the PSS-Na coated active layer were (107.9 ± 0.3)° and (99.0 ± 0.2)°, respectively (see Figure S1, Supporting Information). The PSS-Na coated active layer became more hydrophilic than without PSS-Na. AFM was used to investigate the surface morphology of the PAL with and without the PSS-Na layer. The AFM image (Figure S2, Supporting Information) of the PAL without the PSS-Na film showed clearly P3HT-rich and PCBM-rich domains due to phase separation behavior. The image of the PAL with PSS-Na showed quite different features. This is due to that the PSS-Na layer covers the roughness of the PAL surface. The surface roughness (Figure S2, Supporting Information) of the PSS-Na coated active layer (P3HT:PCBM) is smoother than that of the active layer wihout PSS-Na. This means that the PSS-Na film can form uniformly on the active layer.

PLED and PSC Properties. We fabricated a series of PLEDs with the PSS-Na film at the EML/Al interface to investigate the effect of the PSS-Na film on the devices. To compare the performances of the devices with the PSS-Na as an IFL, we also fabricated the PLEDs without IFL and with a 0.5 nm thick LiF film as an IFL. Figure 3 shows the characteristics of a series of PLEDs with or without an IFL. The performances of the PLEDs are summarized in Table 1. The typical diode characteristics were observed in all the devices. As shown in Figure 3d, the electroluminescent (EL) spectrum of the device with IFL0.5 was almost identical to that of the device without IFL. One can easily notice that the devices with the PSS-Na film as an IFL exhibited better electron transporting ability than that of the devices without IFL. We varied the thickness of the IFL to optimize the device performances by varying the concentration of PSS-Na solutions. We refer to the spin-coated PSS-Na film from the concentrations of 0.1, 0.5, and 1.0 mg/mL as IFL0.1, IFL0.5, and IFL1.0, respectively. However, we could not measure the thickness of the PSS-Na film directly on the EML or PAL by using a thickness monitor (Alpha-Step IQ surface profiler) or an AFM because the surface roughness of the PAL (see Figure S2, Supporting Information) is comparable to the thickness of the PSS-Na film. Therefore, we measured the thickness of films on silicon wafers by using ellipsometry. The thickness of PSS-Na film was measured according to the literature procedures.[16] The PSS-Na films were prepared under the same spin-coating condition as in the device fabrications. The thicknesses of PSS-Na layers prepared from the concentrations of 0.1, 0.5, and 1.0 mg/mL were 2.44 ± 0.04, 4.08 ± 0.05, and 4.68 ± 0.15 nm, respectively. Even though the surface property of the PAL (or EML) is different from that of the Si wafer, the thickness of the PVA film on the PAL (or EML) would be similar to those on the Si wafer.

The device without an IFL (ITO/PEDOT/PF9B/Al) showed a turn-on voltage (V_{on}) of 9.5 V, a maximum luminance efficiency (LE_{max}) of 0.316 cd/A, and a maximum brightness (B_{max}) of 476 cd/m^2, respectively. Contrarily, the device with an IFL0.5 exhibited a V_{on} of 5.5 V, a LE_{max} of 3.00 cd/A, and a B_{max} of 4348 cd/m^2, respectively, which are dramatically improved than those of the device without an IFL. Besides, the V_{on} and the LE_{max} are comparable to those of the device with 0.5 nm thick LiF (V_{on} = 6.0 V, LE_{max} = 3.64 cd/A). As shown in Figure 3 and Table 1, the performances of PLEDs were dependent on the concentration of the PSS-Na solution. The LE_{max} of the devices with an IFL1.0 exhibited a relatively high efficiency. The performances of the device with an IFL0.1 were very poor, which are close to the performances of the device without an IFL. One possible reason for the poor performances is that the EML is not fully covered with the PSS-Na. As for the device with an IFL1.0, the PSS-Na film was too thick, leading to decreased current density, B_{max}, and increased V_{on}. The V_{on} values of the devices with the PSS-film as an IFL were smaller than that of the device without an IFL, indicating that the electron injection process is facilitated by the PSS-Na film. Even though the reduction of a Schottky barrier was small, the electron transporting/injecting properties are improved by the insertion of the PSS-Na film between the EML and the cathode. The devices in this research seem to need to be optimized further because the V_{on} values of the devices were higher than previously reported data.[29] However, one can notice that the performances (V_{on}, LE, and B) of the devices with the PSS-Na film are better than those of the device without PSS-Na.

A series of PSCs with the PSS-Na film at the PAL/Al were fabricated to investigate the effect of the PSS-Na film on the

devices. To compare the performances of the devices, we also fabricated the PSCs without an IFL and with a 1.0 nm thick LiF film as an IFL. Figure 4a shows the photovoltaic characteristics

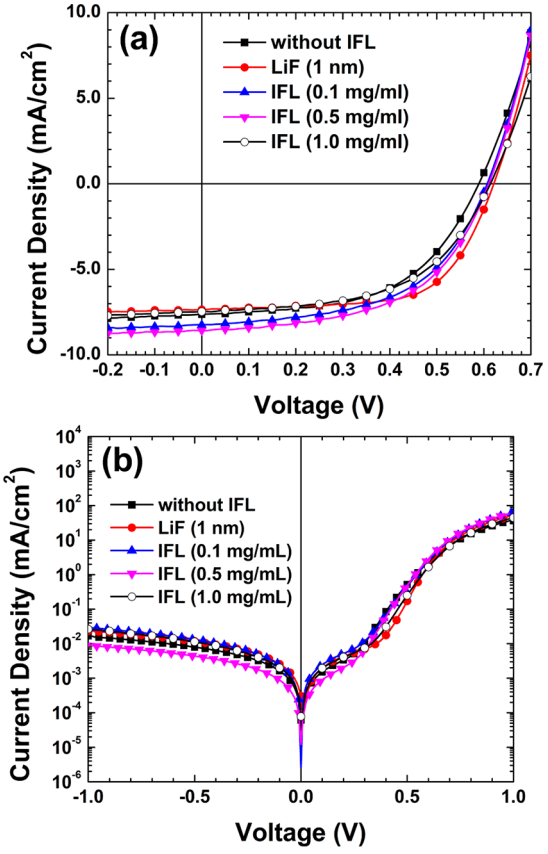

Figure 4. Current density−voltage curves of PSCs (a) under AM 1.5G simulated illumination with an intensity of 100 mW/cm^2 and (b) under the dark condition (filled rectangle: without IFL; filled circle: a 1.0 nm thick LiF as an IFL; filled triangle: PSS-Na coated from the solution of 0.1 mg/mL; filled reverse triangle: PSS-Na coated from the solution of 0.5 mg/mL; circle: PSS-Na coated from the solution of 1.0 mg/mL).

of the PSCs with the PSS-Na film as an IFL with a configuration of ITO/PEDOT:PSS/PAL/IFL/Al. The photovoltaic parameters are summarized in Table 2. The power conversion efficiency (PCE) of the device with an IFL0.5 was 2.83%, which is a 16% increase compared to that of the device without an IFL. Most of the increase in the device efficiency resulted from the 12% enhancement in the short-circuit current (J_{sc}), while the fill factor (FF) was very close to that of the device without an IFL. This result is not usually observed in the previously reported results of the buffer layer based on PEO,[16] CPEs,[17−20] P-OH,[21] and PVs,[22,23] for which either the J_{sc} and the FF increase simultaneously or only the FF increases along with the increase of the V_{oc}.

For the devices with an IFL0.1, the J_{sc} and the PCE were −8.25 mA/cm^2 and 2.69%, respectively, which is an increase of 8% of J_{sc} and a 10% of PCE compared to those of the device without an IFL. The FF of the device with IFL0.1 shows a similar feature with the device with IFL0.5. The performances of the device with an IFL0.5 and IFL0.1 are improved than those of the device without an IFL, while the PCE of the device with an IFL1.0 is comparable to that of the device without PSS-Na. The PCE of the device with an IFL0.5 was very comparable to that of the device with 1.0 nm thick LiF at the PAL/Al interface. The PCE of the device with an IFL0.5 was very comparable to that of the device with 1.0 nm thick LiF at the PAL/Al interface. The V_{oc} values of all the devices with the PSS-NA film were 0.61 V, which are slightly improved than that of the device without IFL. This is presumably due to that the reduction of a Schottky barrier is small (ca. 0.1 eV). This is a different result from the cases of the reported IFLs based on PEO,[16] CPEs,[17−20] P-OH,[21] and PVs,[22,23] for which the large increase of V_{oc} was attributed to the enhancement of the PCE of the devices. Recently, Wang et al. reported a similar observation in the device with poly(vinylpyrrolidone) (PVP) as an IFL,[37] which is a nonconjugated neutral polymer with a strong dipole moment.

In general, current density−voltage curves under the dark condition provide information about the series resistance (R_s) and the parallel resistance (R_p), which were calculated from the inverse slope near the high current regime and the slope near the lower current region in the dark $J-V$ curves, respectively. As shown in Figure 4b and Table 2, the R_s and R_p values of the devices with an IFL0.1 and IFL1.0 were smaller than those of the device without an IFL, and these are coincident with the higher current density for the devices with PSS-Na at both the reverse and the forward bias in the dark. The device with an IFL0.5 showed a smaller R_s value and a larger R_p value compared with those of the device without PSS-Na, whereas IFL0.1 and IFL1.0 exhibited smaller R_s and R_p values. Interestingly, the FF value of the device with IFL0.5 is very similar to that of the device without PSS-Na, regardless of the improvement in R_s and R_p values of the device with IFL0.5. As mentioned before, this result is different from the previously reported result of the buffer layers, such as PEO, CPEs, and P-OH. The J_{sc} depends on the multiplication of the photoinduced charge carrier density, the charge carrier mobility in the active layer, the interface properties at the interfaces (i.e., between the PAL and the electrodes), and charge trasnport.[37,38] The improvement of J_{sc} is mainly due to that the reduction of work function of the cathode increases the built-in potential of the solar cells, which also increases the extraction field when the

Table 2. Summary of Photovoltaic Parameters of PSCs with the Best PCE Value[a]

	V_{oc} (V)	J_{sc} (mA/cm^2)	FF (%)	PCE (%)	R_s (Ω cm^2)[b]	R_p (kΩ cm^2)[c]
without IFL	0.59 (0.59 ± 0.01)	−7.64 (−7.59 ± 0.21)	54.1 (54.5 ± 1.67)	2.44 (2.43 ± 0.95)	5.76	62.8
LiF (1 nm)	0.62 (0.62 ± 0.01)	−7.35 (−7.43 ± 0.08)	64.7 (64.1 ± 0.65)	2.95 (2.95 ± 0.03)	2.77	43.0
IFL (0.1 mg/mL)	0.61 (0.61 ± 0.01)	−8.25 (−8.20 ± 0.07)	53.5 (53.8 ± 0.28)	2.69 (2.67 ± 0.03)	2.63	33.9
IFL (0.5 mg/mL)	0.61 (0.61 ± 0.01)	−8.58 (−8.32 ± 0.10)	54.0 (54.7 ± 0.24)	2.83 (2.77 ± 0.07)	3.39	113
IFL (1.0 mg/mL)	0.61 (0.62 ± 0.01)	−7.47 (−7.41 ± 0.10)	54.7 (54.2 ± 0.28)	2.49 (2.47 ± 0.04)	3.48	38.7

[a]The averages for photovoltaic parameters of each device are given in parentheses with mean variation. [b]The series resistance (estimated from the device with the best PCE value). [c]The parallel resistance (estimated from the device with the best PCE value).

device is biased at the short-circuit condition. In our results, the PSS-Na layer plays an important role in improving the interface properties (i.e., improved Ohmic contact at the interfaces). Therefore, it is plausible that the higher J_{sc} values of the devices with the PSS-Na layer are related to the enhanced charge tranport to the cathode. The incident photon conversion efficiency (IPCE) spectra (Figure S3, Supporting Information) of the devices are coincident with the higher PCE for the device with PSS-Na. This also supports that the device with PSS-Na shows better performances than the device without PSS-Na.

CONCLUSION

We have demonstrated an anionic nonconjugated polyelectrolyte, PSS-Na, to modify the property at the organic/Al interface in both PLEDs and PSCs. The UPS and KPM studies indicate that a Schottky barrier between the organic layer and the Al cathode is reduced by the formation of a favorable interface dipole by the PSS-Na film. The performances of PLEDs and PSCs depend on the thickness of the PSS-Na film. The PLED and PSC with the PSS-Na film spin-coated from a solution of 0.5 mg/mL showed the best performances, which are higher than those of the device without the PSS film. This research provides a very simple and facile strategy for the enhancement of the efficiency of the optoelectronic devices.

ASSOCIATED CONTENT

Supporting Information

The water contact angle data, the surface morphology of the active layer with and without the PSS-Na film, and IPCE spectra of PSCs are available in the Supporting Information. This material is available free of charge via the Internet at http://pubs.acs.org.

AUTHOR INFORMATION

Corresponding Author

*E-mail: jkim@pknu.ac.kr.

Notes

The authors declare no competing financial interest.

ACKNOWLEDGMENTS

This research was supported by the Converging Research Center Program through the Ministry of Education, Science and Technology (2012K001279) and Basic Science Research Program through the National Research Foundation of Korea (NRF) funded by the Ministry of Education, Science and Technology (2013020225).

REFERENCES

(1) Yu, G.; Gao, J.; Hummelen, J. C.; Wudl, F.; Heeger, A. J. *Science* **1995**, *270*, 1789−1791.
(2) Huynh, W. U.; Dittmer, J. J.; Alivisatos, A. P. *Science* **2002**, *295*, 2425−2427.
(3) Gunes, S.; Neugebauer, H.; Sariciftci, N. S. *Chem. Rev.* **2007**, *107*, 1324−1338.
(4) Friend, R. H.; Gymer, R. W.; Holmes, A. B.; Burroughes, J. H.; Marks, R. N.; Taliani, C.; Bradley, D. D. C.; Dos Santos, D. A.; Brédas, J. L.; Lögdlund, M.; Salaneck, W. R. *Nature* **1999**, *397*, 121−128.
(5) Thompson, B. C.; Fréchet, J. M. J. *Angew. Chem., Int. Ed.* **2007**, *47*, 58−77.
(6) de Jong, M. P.; van Ijzendoorn, L. J.; de Voigt, M. J. A. *Appl. Phys. Lett.* **2000**, *77*, 2255−2257.
(7) Zhang, F. L.; Johansson, M.; Andersson, M. R.; Hummelen, J. C.; Inganas, O. *Adv. Mater.* **2002**, *14*, 662−665.
(8) Bacher, E.; Bayerl, M.; Rudati, P.; Reckefuss, N.; Muller, C. D.; Meerholz, K.; Nuyken, O. *Macromolecules* **2005**, *38*, 1640−1643.
(9) Jungermann, S.; Riegel, N.; Muller, D.; Meerholz, K.; Nuyken, O. *Macromolecules* **2006**, *39*, 8911−8911.
(10) Liu, S.; Jiang, X.; Ma, H.; Liu, M.-S.; Jen, A. K. -Y. *Macromolecules* **2000**, *33*, 3514−3517.
(11) Liu, M.-S.; Niu, Y.-H.; Ka, J.-W.; Yip, H.-L.; Huang, F.; Luo, J.; Kim, T.-D.; Jen, A. K.-Y. *Macromolecules* **2008**, *41*, 9570−9580.
(12) Lim, Y.; Park, Y.-S.; Kang, Y.; Jang, D. Y.; Kim, J. H.; Kim, J.-J.; Sellinger, A.; Yoon, D.-Y. *J. Am. Chem. Soc.* **2011**, *133*, 1375−1382.
(13) Khodabakhsh, S.; Sanderson, B. M.; Nelson, J.; Jones, T. S. *Adv. Funct. Mater.* **2006**, *16*, 95−100.
(14) Goh, C.; Scully, S. R.; McGehee, M. D. *J. Appl. Phys.* **2007**, *101*, 114503.
(15) Kang, H.; Hong, S.; Lee, J.; Lee, K. *Adv. Mater.* **2012**, *24*, 3005−3009.
(16) Zhang, F.; Ceder, M.; Inganas, O. *Adv. Mater.* **2007**, *19*, 1835−1838.
(17) Choi, H.; Park, J. S.; Jeong, E.; Kim, G.-W.; Lee, B. R.; Kim, S. O.; Song, M. H.; Woo, H. Y.; Kim, J. Y. *Adv. Mater.* **2011**, *23*, 2759−2763.
(18) Oh, S.-W.; Na, S.-I.; Jo, J.; Lim, B.; Vak, D.; Kim, D.-Y. *Adv. Funct. Mater.* **2010**, *20*, 1977−1983.
(19) Ma, W.; Iyer, P. K.; Gong, X.; Kiu, B.; Moses, D.; Bazan, G. C.; Heeger, A. J. *Adv. Mater.* **2005**, *17*, 274−277.
(20) Na, S.-I.; Oh, S.-H.; Kim, S.-S.; Kim, D.-Y. *Org. Electron.* **2009**, *10*, 496−500.
(21) Huang, F.; Zhang, Y.; Liu, M.-S.; Jen, A. K.-Y. *Adv. Funct. Mater.* **2009**, *19*, 2457−2466.
(22) Jo, M. Y.; Ha, Y. E.; Kim, J. H. *Sol. Energy Mater. Sol. Cells* **2012**, *107*, 1−8.
(23) Jo, M. Y.; Ha, Y. E.; Kim, J. H. *Org. Electron.* **2013**, *14*, 995−1001.
(24) Kim, J. Y.; Kim, S. H.; Lee, H.-H.; Lee, K.; Ma, W.; Gong, X.; Heeger, A. J. *Adv. Mater.* **2006**, *18*, 572−576.
(25) Seo, H. O.; Park, S.-Y.; Shim, W. H.; Kim, K.-D.; Lee, K. H.; Jo, M. Y.; Kim, J. H.; Lee, E.; Kim, D.-W.; Kim, Y. D.; Lim, D. C. *J. Phys. Chem. C* **2011**, *115*, 21517−21520.
(26) Zhu, X.; Xie, Y.; Li, X.; Qiao, X.; Wang, L.; Tu, G. *J. Mater. Chem.* **2012**, *22*, 15490−15494.
(27) Jin, Y.; Bazan, G. C.; Heeger, A. J.; Kim, J. Y.; Lee, K. *Appl. Phys. Lett.* **2008**, *93*, 1233041.
(28) Decher, G.; Hong, J. D.; Schmitt, J. *Thin Solid Films* **1992**, *210/211*, 831−835.
(29) Herguth, P.; Jiang, X.; Liu, M. S.; Jen, A. K.-Y. *Macromolecules* **2002**, *35*, 6094−6100.
(30) Ishii, H.; Sugiyama, K.; Ito, E.; Seki, K. *Adv. Mater.* **1999**, *11*, 605−625.
(31) Braun, S.; Salaneck, W.; Fahlman, M. *Adv. Mater.* **2009**, *21*, 1450−1472.
(32) Bruening, M.; Moons, E.; Cahen, D.; Shanzer, A. *J. Phys. Chem.* **1995**, *99*, 8368−8373.
(33) Bastide, S.; Butruille, R.; Cahen, D.; Dutta, A.; Libman, J.; Shanzer, A.; Sun, L.; Vilan, A. *J. Phys. Chem. B* **1997**, *101*, 2678−2684.
(34) Ha, Y. E.; Jo, M. Y.; Park, J.; Kang, Y.-C.; Yoo, S. I.; Kim, J. H. *J. Phys. Chem. C* **2013**, *117*, 2646−2652.
(35) Chang, Y.-M.; Zhu, R.; Richard, E.; Chen, C.-C.; Li, G.; Yang, Y. *Adv. Funct. Mater.* **2012**, *22*, 3284−3289.
(36) Zhu, X.; Xie, Y.; Li, X.; Qiao, X.; Wang, L.; Tu, G. *J. Mater. Chem.* **2012**, *22*, 15490−15494.
(37) Wang, H.; Zhang, W.; Xu, C.; Bi, X.; Chen, B.; Wang, S. *ACS Appl. Mater. Interfaces* **2013**, *5*, 26−34.
(38) Kang, J.-W.; Lee, S.-P.; Kim, D.-G.; Lee, S.; Lee, G.-H.; Kim, J.-K.; Park, S.-Y.; Kim, J. H.; Kim, H.-K.; Jeong, Y.-S. *Electrochem. Solid-State Lett.* **2009**, *12*, H64−H66.